

# Point Collocation Method Based on the FMLSrk Approximation for Electromagnetic Field Analysis

Do Wan Kim and Hong-Kyu Kim

**Abstract**—This paper presents the methodology of a mesh-free point collocation method and its application to the electromagnetic field computation. The special emphasis in this paper is on a point collocation scheme based on the fast moving least square reproducing kernel (FMLSrk) method with a variable dilation function. The concept of dilation function is newly introduced here, and we combine it with the conventional FMLSrk method. They yield the FMLSrk approximation operators. In the point collocation method using such an extended FMLSrk method, there is no need to construct integration cells, and any type of boundary conditions can be directly enforced. Numerical simulations for a two-dimensional (2-D) electromagnetic field on complicated geometry are carried out to validate the reliability of proposed method, in which the dilation function plays an essential role.

**Index Terms**—Dilation function, electromagnetic field, extended FMLSrk, point collocation.

## I. INTRODUCTION

SEVERAL kinds of meshfree point collocation methods have been successfully applied to the analysis of the mechanical problems [1]–[3]. The shape functions in many mesh-free methods are derived from the moving least square reproducing kernel (MLSrk) approximation [4], [5]. Although almost all kinds of meshfree methods including MLSrk method have been developed extensively as potential methodologies, there are two important problems that still need improvement. One is to reduce the computational cost of the derivatives of shape functions, and the other is to allow the dilation parameter to vary not only at nodes but also at the other points with the consistency conditions that are still satisfied. As a solution for the former, we will take the fast moving least square reproducing kernel (FMLSrk) method [6], and for the latter, the notion of a dilation function will be newly introduced, where the name of dilation function comes from the varying dilation parameter mentioned above. Then, combining the dilation function with the FMLSrk method, we can propose the extended fast moving least square reproducing kernel method. For completeness of the paper, constructing the dilation function should be included.

Last, the point collocation method based on the extended FMLSrk method is presented. Since point collocation methods attack the strong form of the governing equations in general, fast

calculations of higher order derivatives of shape functions are needed in discretization. Furthermore, since singular behaviors of the solution may take place on a complicated geometry, the irregular node distributions are essential for an accurate solution. From those reasons, the extended FMLSrk method is suitable to the point collocation method, which produces the approximate derivatives of shape functions instead of real derivatives.

Besides easy discretization of the governing equation, the salient feature among the merits of point collocation methods is flexibility in implementing boundary conditions. Because the shape functions do not have the Kronecker delta condition, special treatment for the boundary conditions is required, for example, using the D'Alembert principle or the Lagrange multiplier method is typical. However, in the point collocation method, roughly speaking, any kind of boundary conditions can be directly enforced theoretically.

By some numerical experiments, the rate of convergence and the accuracy of the method are shown, and we perform the numerical computation of the electric potential on a complicated geometry in which a geometric singularity is located.

## II. EXTENDED FAST MOVING LEAST SQUARE REPRODUCING KERNEL METHOD

Let  $\Omega$  be a bounded domain in  $\mathbb{R}^n$ , and let  $\Lambda \equiv \{\mathbf{x}_I \in \overline{\Omega} | I = 1, \dots, N\}$  be a set of distributed nodes in  $\overline{\Omega}$ . Throughout the paper, multi-index notations and related definitions are employed as follows:

$$\begin{aligned} \alpha &= (\alpha_1, \dots, \alpha_n), & \mathbf{x} &= (x_1, x_2, \dots, x_n) \in \mathbb{R}^n \\ |\alpha| &\equiv \sum_{i=1}^n \alpha_i, & \alpha! &\equiv \alpha_1! \alpha_2! \dots \alpha_n! \\ \mathbf{x}^\alpha &\equiv x_1^{\alpha_1} x_2^{\alpha_2} \dots x_n^{\alpha_n}, & D_{\mathbf{x}}^\alpha &\equiv \partial_{x_1}^{\alpha_1} \partial_{x_2}^{\alpha_2} \dots \partial_{x_n}^{\alpha_n} \end{aligned}$$

where  $\alpha_k$ 's are non-negative integers, and  $\alpha$  is called the multi-index. We first consider the vector of complete basis polynomials in  $\mathbb{R}^n$  up to order  $m$  such that

$$\mathbf{P}_m(\mathbf{x}) = (\mathbf{x}^{\beta_1}, \mathbf{x}^{\beta_2}, \dots, \mathbf{x}^{\beta_L})^T, \quad L = \frac{(m+n)!}{m!n!} \quad (1)$$

where  $\beta_k$ 's are all multi-indexes in lexicographical order.

Let  $B_r(\mathbf{z}) \equiv \{\mathbf{y} | \|\mathbf{y} - \mathbf{z}\| < r\}$  be the  $r$ -ball in  $\mathbb{R}^n$  with center  $\mathbf{z}$ . We introduce the continuous non-negative window function with its support on  $\overline{B_1(\mathbf{0})}$  of the type

$$\Phi(\mathbf{x}) = (1 - \|\mathbf{x}\|)^4, \quad \text{for } \|\mathbf{x}\| < 1, \mathbf{x} \in \mathbb{R}^n$$

and the continuous positive dilation function

$$\rho(\mathbf{x}) > 0 \quad \text{on } \overline{\Omega}.$$

Manuscript received July 1, 2003. This work was supported by the Basic Research Program of the Korea Science and Engineering Foundation under Grant R05-2003-000-10427-0.

D. W. Kim is with the Department of Mathematics, Sunmoon University, Choong-nam, Korea (e-mail: dwkim@webmail.sunmoon.ac.kr).

H.-K. Kim is with Korea Electrotechnology Research Institute, Changwon, 641-120, Korea (e-mail: kimhk@keri.re.kr).

Digital Object Identifier 10.1109/TMAG.2004.824612

From now on, we use brief notation  $\rho_{\mathbf{x}}$  instead of  $\rho(\mathbf{x})$  if there is no confusion. The support of the window function has the shape of  $n$ -dimensional unit ball. The dilation parameter commonly used in most meshfree methods is about to be replaced with the dilation function  $\rho_{\mathbf{x}}$ . Here we note that the continuity of the dilation function is enough to combine the dilation function with the FMLSrk method.

We assume that  $\rho_{\mathbf{x}}$  is chosen such that the number of nodes contained in  $B_{\rho_{\mathbf{x}}}(\mathbf{x})$  is greater than  $L$ . The construction of such  $\rho_{\mathbf{x}}$  will be addressed in Section III. With the window function  $\Phi(\mathbf{x})$  and such dilation function  $\rho_{\mathbf{x}}$ , we find the vector  $\mathbf{a}$  to minimize the following weighted square functional at  $\bar{\mathbf{x}} \in \bar{\Omega}$

$$J(\mathbf{a}; \bar{\mathbf{x}}, u) \equiv \sum_{\mathbf{x}_I \in \Lambda} |u(\mathbf{x}_I) - \mathbf{U}_m^{\rho_{\mathbf{x}}}(\mathbf{x}_I; \bar{\mathbf{x}}, \mathbf{a})|^2 \Phi\left(\frac{\mathbf{x}_I - \bar{\mathbf{x}}}{\rho_{\bar{\mathbf{x}}}}\right) \quad (2)$$

where  $u(\mathbf{x})$  is a continuous function defined in  $\bar{\Omega}$ , and  $\mathbf{U}_m^{\rho_{\mathbf{x}}}(\mathbf{x}; \bar{\mathbf{x}}, \mathbf{a}) \equiv \mathbf{P}_m(\mathbf{x} - \bar{\mathbf{x}}/\rho_{\bar{\mathbf{x}}}) \cdot \mathbf{a}$ . Then, the minimizer  $\mathbf{a}$  should be a function of  $\bar{\mathbf{x}}$  and  $u$ , and we can make the following approximation operators for  $u$  by limiting process:

$$D_{m, \rho_{\mathbf{x}}}^{\beta_k} u(\mathbf{x}) \equiv \lim_{\bar{\mathbf{x}} \rightarrow \mathbf{x}} D_{\mathbf{x}}^{\beta_k} \mathbf{U}_m^{\rho_{\mathbf{x}}}(\mathbf{x}; \bar{\mathbf{x}}, \mathbf{a}(\bar{\mathbf{x}}, u)), \quad |\beta_k| \leq m.$$

As a matter of fact, the operators  $D_{m, \rho_{\mathbf{x}}}^{\beta_k}$ 's are linear in  $u(\mathbf{x})$ . We call the operator  $D_{m, \rho_{\mathbf{x}}}^{\beta}$  ( $|\beta| \leq m$ ) the  $\beta$ th FMLSrk operator with respect to  $\rho_{\mathbf{x}}$ .

Suppose  $\{u_I(\mathbf{x}) | u_I(\mathbf{x}_I) = \delta_{IJ}, \mathbf{x}_I, \mathbf{x}_J \in \Lambda\}$  is a set of continuous functions. We define the following functions:

$$\Psi_I^{\rho_{\mathbf{x}}, [\beta_k]}(\mathbf{x}) \equiv D_{m, \rho_{\mathbf{x}}}^{\beta_k} u_I(\mathbf{x}).$$

Then, the functions  $\Psi_I^{\rho_{\mathbf{x}}, [\beta_k]}(\mathbf{x})$  result in the solutions of the following equations:

$$M^{\rho_{\mathbf{x}}}(\mathbf{x}) \begin{pmatrix} \frac{\rho_{\mathbf{x}}^{|\beta_1|}}{\beta_1!} \Psi_I^{\rho_{\mathbf{x}}, [\beta_1]}(\mathbf{x}) \\ \frac{\rho_{\mathbf{x}}^{|\beta_2|}}{\beta_2!} \Psi_I^{\rho_{\mathbf{x}}, [\beta_2]}(\mathbf{x}) \\ \vdots \\ \frac{\rho_{\mathbf{x}}^{|\beta_L|}}{\beta_L!} \Psi_I^{\rho_{\mathbf{x}}, [\beta_L]}(\mathbf{x}) \end{pmatrix} = \mathbf{P}_m\left(\frac{\mathbf{x}_I - \mathbf{x}}{\rho_{\mathbf{x}}}\right) \Phi\left(\frac{\mathbf{x}_I - \mathbf{x}}{\rho_{\mathbf{x}}}\right) \quad (3)$$

where  $M^{\rho_{\mathbf{x}}}(\mathbf{x})$  is called the moment matrix and is defined such that

$$M^{\rho_{\mathbf{x}}}(\mathbf{x}) \equiv \sum_{\mathbf{x}_I \in \Lambda} \mathbf{P}_m\left(\frac{\mathbf{x}_I - \mathbf{x}}{\rho_{\mathbf{x}}}\right) \mathbf{P}_m^T\left(\frac{\mathbf{x}_I - \mathbf{x}}{\rho_{\mathbf{x}}}\right) \Phi\left(\frac{\mathbf{x}_I - \mathbf{x}}{\rho_{\mathbf{x}}}\right). \quad (4)$$

We call the function  $\Psi_I^{\rho_{\mathbf{x}}, [\beta]}$  ( $\mathbf{x}$ ), the  $\beta$ th shape function associated with the window function  $\Phi$  and the dilation function  $\rho_{\mathbf{x}}$  or, briefly, call it the  $\beta$ th shape function if no confusion arises. The following properties of the  $\beta$ th FMLSrk operator can be justified by slight modification of the proof in the literature [6].

- 1) (Generalized  $m$ th-Order Consistency) The  $\beta$ th FMLSrk operator  $D_{m, \rho_{\mathbf{x}}}^{\beta}$  is exactly same as the differential operator  $D^{\beta}$  on the polynomial space up to order  $m$ , i.e.,

$$D_{m, \rho_{\mathbf{x}}}^{\beta} u(\mathbf{x}) = D^{\beta} u(\mathbf{x}), \quad |\beta| \leq m \quad (5)$$

whenever  $u(\mathbf{x})$  is a polynomial of order up to  $m$ .

- 2) (Truncation Error between  $D_{m, \rho_{\mathbf{x}}}^{\beta}$  and  $D^{\beta}$ ) Assume the window function  $\Phi(\mathbf{x}) \in C_0^0(\mathbb{R}^n)$  and  $v(\mathbf{x}) \in C^{m+1}(\bar{\Omega})$ , where  $\Omega$  is a bounded open convex set in  $\mathbb{R}^n$ . If there exist the node set  $\Lambda$  and its corresponding  $\rho_{\mathbf{x}}$  to satisfy the following estimate when  $|\beta| \leq m$ :

$$\left| N_{\rho_{\mathbf{x}}}(\mathbf{x}) \frac{\rho_{\mathbf{x}}^{|\beta|}}{\beta!} \Psi_I^{\rho_{\mathbf{x}}, [\beta]}(\mathbf{x}) \right| < C$$

for some constant  $C$  independent of  $\rho_{\mathbf{x}}$ , where  $N_{\rho_{\mathbf{x}}}(\mathbf{x})$  is the number of nodes contained in  $B_{\rho_{\mathbf{x}}}(\mathbf{x})$  and  $m$  and  $p$  satisfy  $m > (n/p) - 1$ , then the following estimate holds for  $|\beta| \leq m$  and some constant  $C$  independent of  $\rho_{\Omega}$ :

$$\|D^{\beta} v - D_{m, \rho_{\mathbf{x}}}^{\beta} v\|_{L^p(\Omega)} \leq C \rho_{\Omega}^{m+1-|\beta|} \|v\|_{W^{m+1, p}(\Omega)} \quad (6)$$

where  $\rho_{\Omega} = \sup_{\mathbf{x} \in \Omega} \rho_{\mathbf{x}}$ .

These properties tell us that the  $\beta$ th FMLSrk operator  $D_{m, \rho_{\mathbf{x}}}^{\beta}$  is a good approximation of the derivative  $D^{\beta}$ .

### III. CONSTRUCTION OF CONTINUOUS DILATION FUNCTION $\rho_{\mathbf{x}}$

We start with rough explanation of the idea to construct the continuous dilation function for each point. Initially, choose tentative probe ball  $B_r(\mathbf{x})$ , which contains sufficiently many  $N_s^*$  of nodes, say  $N_s^* > ((m+n)!/m!n!)$ . Then, we define the continuous pseudo-density function  $\delta(\mathbf{x})$  of nodes that are contained in  $B_r(\mathbf{x})$  at each field point  $\mathbf{x}$ . The reciprocal of the density function ( $1/\delta(\mathbf{x})$ ) corresponds to the occupying average pseudo-volume per one node in the ball. Now, we choose the desired number  $N_d$ ,  $((m+n)!/m!n!) < N_d < N_s^*$  of nodes that hopefully belonging to the ball  $B_{\rho_{\mathbf{x}}}(\mathbf{x})$ . Note that  $N_d > ((m+n)!/m!n!)$  is required for the invertibility of the moment matrix for suitably distributed nodes. For stable  $\rho_{\mathbf{x}}$ , we usually take  $N_d = K \times ((m+n)!/m!n!)$  for some  $K > 1$ . Finally, we determine  $\rho_{\mathbf{x}}$  so that the volume of  $B_{\rho_{\mathbf{x}}}(\mathbf{x})$  is equal to  $(N_d/\delta(\mathbf{x}))$ . The following are the details of the construction of  $\rho_{\mathbf{x}}$ .

Let  $\Lambda$  be the set of  $N$  nodes, let  $\mathbf{x}$  be a field point in  $\bar{\Omega}$ , and define  $\Lambda_{\mathbf{x}}(r) = \{\mathbf{x}_I \in \Lambda | \mathbf{x}_I \in B_r(\mathbf{x})\}$ . The probe radius is chosen by the average distance between  $\mathbf{x}$  and  $\mathbf{x}_I$

$$r = r(\mathbf{x}) \equiv \frac{1}{N} \sum_{\mathbf{x}_I \in \Lambda} \|\mathbf{x} - \mathbf{x}_I\|.$$

Let us define the following pseudo-counting function:

$$N(r, \mathbf{x}) = \sum_{\mathbf{x}_I \in \Lambda} \eta_{B_r(\mathbf{x})}(\mathbf{x}_I)$$

where  $\eta_{B_r(\mathbf{x})}$  is a continuous cut-off function. If  $\eta_{B_r(\mathbf{x})}$  is the characteristic function,  $N(r, \mathbf{x})$  is the exact counting function. Using the exact counting function, it may not be continuous. Hence, in this paper, we choose  $\eta_{B_r(\mathbf{x})}$  as the following for some  $\theta$ ,  $0 \leq \theta < 1$ :

$$\eta_{B_r(\mathbf{x})}(\mathbf{y}) = \begin{cases} 1, & \text{when } \frac{|\mathbf{y}-\mathbf{x}|}{r} < \theta \\ \frac{1}{1-\theta} \left(1 - \frac{|\mathbf{y}-\mathbf{x}|}{r}\right), & \text{when } \theta \leq \frac{|\mathbf{y}-\mathbf{x}|}{r} < 1 \\ 0, & \text{otherwise.} \end{cases} \quad (7)$$

We consider the density function of nodes at  $\mathbf{x} \in \Omega$ , which is defined as the following:

$$\delta(r, \mathbf{x}) = \frac{N(r, \mathbf{x})}{\omega_n r^n} \quad (8)$$

where  $\omega_n$  is the volume of the  $n$ -dimensional unit ball, i.e.,  $\omega_n = |B_1(\mathbf{0})|$ . Note that the reciprocal  $1/(\delta(r, \mathbf{x}))$  is interpreted as the average occupying volume per node in  $\Lambda_{\mathbf{x}}(r)$ . For the enhancement of accuracy for the density function, the following multiprobing is desirable:

$$\delta_c(\mathbf{x}) = \frac{1}{N_c} \sum_{k=1}^{N_c} \delta\left(\frac{r(\mathbf{x})}{2^{k-1}}, \mathbf{x}\right) \quad (9)$$

where  $N_c$  is the number of probing step.

Choose  $N_d$  as the desirable number of nodes that are contained in  $B_{\rho_{\mathbf{x}}}(\mathbf{x})$ . Now, we define the value of the dilation function  $\rho_{\mathbf{x}}$  at each field point as follows:

$$\rho_{\mathbf{x}} = \sqrt[n]{\frac{N_d}{\omega_n \delta_c(\mathbf{x})}}. \quad (10)$$

Although we use the parameters  $\theta = 0$ ,  $K = 3$ , and  $N_c = 3$  frequently throughout the paper, we may have a chance to alter these parameters when the node distribution is highly irregular. In Fig. 1, we see that the support of the shape function and the radial support of the window function at nodes are different when we use concentrated nodes. This does not happen for the case of constant dilation function. At each point  $\mathbf{x}$ , the dilation function  $\rho_{\mathbf{x}}$  determines nodes that contribute to the value of shape function. In fact, the support of the shape function at each node  $\mathbf{x}_I$  is determined in terms of

$$\text{supp} \Psi_I^{\rho_{\mathbf{x}}, [\beta]}(\mathbf{x}) = \overline{\{\mathbf{z} \in \Omega | \mathbf{x}_I \in B_{\rho_{\mathbf{z}}}(\mathbf{z})\}}. \quad (11)$$

Fig. 1 explains above rule determining the support of shape function. In Fig. 1, the 0th shape function is plotted with level curves of the dilation function (normal curves), as proposed in this section. From Fig. 1, we can deduce the intuitive form of the shape function. It is more stiff in the direction of more nodes. Since we designed the dilation function so that each ball  $B_{\rho_{\mathbf{x}}}(\mathbf{x})$  contains almost the same number  $N_d$  of nodes, and the example node set is not concentrated along the boundary, we see a higher level set of dilation functions along the boundary than that of the center in Fig. 2.

#### IV. POINT COLLOCATION SCHEME BASED ON THE FMLSRK OPERATORS

We will propose a point collocation scheme based on the FMLSRK operators. In order to obtain the mesh-free numerical solution of a partial differential equation, we approximate the partial differential operators in the differential equations in terms of the FMLSRK operators. For example, we assume that the following type of Poisson problem is given:

$$-\Delta u = f, \quad \text{on } \Omega \quad (12)$$

$$u = g, \quad \text{on } \Gamma_D \quad (13)$$

$$\frac{\partial u}{\partial n} = h, \quad \text{on } \Gamma_N \quad (14)$$

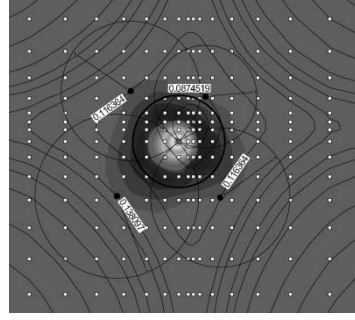


Fig. 1. Comparison between the support of 0th shape function and that of the window function (bold circle).

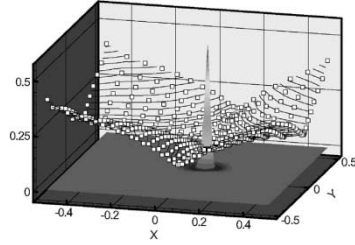


Fig. 2. Plots of the 0th shape function and dilation.

where  $\partial\Omega = \Gamma_D \cup \Gamma_N$ , and  $\Gamma_D \cap \Gamma_N = \phi$ . Using the FMLSRK operators, it can be translated into the following point collocation approximation:

$$-\left(D_{m, \rho_{\mathbf{x}}}^{(2,0)} + D_{m, \rho_{\mathbf{x}}}^{(0,2)}\right) u = f, \quad \text{on } \Lambda_i \quad (15)$$

$$D_{m, \rho_{\mathbf{x}}}^{(0,0)} u = g, \quad \text{on } \Lambda_d \quad (16)$$

$$\mathbf{n} \cdot \left(D_{m, \rho_{\mathbf{x}}}^{(1,0)}, D_{m, \rho_{\mathbf{x}}}^{(0,1)}\right) u = h, \quad \text{on } \Lambda_n \quad (17)$$

where  $\Lambda = \Lambda_i \cup \Lambda_d \cup \Lambda_n$ , and  $\Lambda_i$ ,  $\Lambda_d$ , and  $\Lambda_n$  are sets of interior nodes, Dirichlet boundary nodes, and Neumann boundary nodes, respectively. Here,  $\mathbf{n}$  is the outward unit normal vector at  $\mathbf{x}^n \in \Lambda_n$ . The truncation error is of order  $O(\rho_{\Omega}^{m-1})$ . Thus, in this case, we need  $m \geq 2$  for convergence. For the stable solution, the diagonal preconditioning is adopted, and the resultant discrete equations from the point collocation (15)–(17) are addressed as in the following:

$$-\sum_{\mathbf{x}_J \in \Lambda} u(\mathbf{x}_J) \rho^2 \left( \Psi_J^{\rho_{\mathbf{x}}, [(2,0)]} + \Psi_J^{\rho_{\mathbf{x}}, [(0,2)]} \right) = \rho^2 f, \quad \text{on } \Lambda_i$$

$$\sum_{\mathbf{x}_J \in \Lambda} u(\mathbf{x}_J) \Psi_J^{\rho_{\mathbf{x}}, [(0,0)]} = g, \quad \text{on } \Lambda_d$$

$$\sum_{\mathbf{x}_J \in \Lambda} u(\mathbf{x}_J) \rho \left( \Psi_J^{\rho_{\mathbf{x}}, [(1,0)]}, \Psi_J^{\rho_{\mathbf{x}}, [(0,1)]} \right) \cdot \mathbf{n} = \rho h, \quad \text{on } \Lambda_n$$

where  $\rho$  is the dilation function. Solving this linear system for the unknowns  $u(\mathbf{x}_J)$ 's, we can build up the approximate solution and its derivatives via the approximations

$$D_{m, \rho_{\mathbf{x}}}^{\beta} u = \sum_{\mathbf{x}_J \in \Lambda} u(\mathbf{x}_J) \Psi_J^{\rho_{\mathbf{x}}, [\beta]}(\mathbf{x}), \quad |\beta| \leq m. \quad (18)$$

The adequate dilation function for irregular node distribution is expected to play an essential role in treating the geometric singularities.

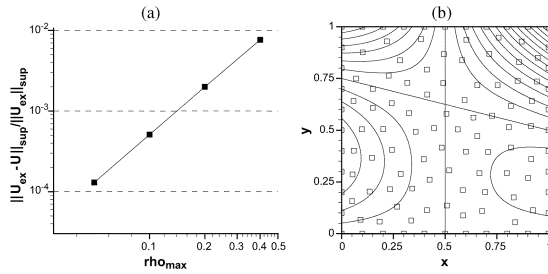


Fig. 3. (a) Convergence test for uniform node sets ( $10 \times 10$ ,  $20 \times 20$ ,  $40 \times 40$ ,  $80 \times 80$ ) when  $m = 2$  and (b) exactly reproduced polynomial solution even on random nodes ( $114 - \square$ ) when  $m = 3$ .

## V. NUMERICAL VALIDATION OF POINT COLLOCATION SCHEME

We take the electrostatic problem into consideration as an application of our method. The electric potential function  $V(x, y)$  is governed by Poisson type of partial differential equations of (12)–(14). Before dealing with a complicated example, we are going to show the accuracy and convergence of the scheme by comparing the numerical solution to the exact one. We choose a cubic polynomial as the exact solution of the Poisson problem on the unit square  $[0,1] \times [0,1]$  as the following:

$$u(x, y) = -y(2x - 1)(x + 4y - 3)$$

and its corresponding force term  $f(x, y)$  becomes the linear polynomial  $-16x - 4y + 8$ . On the lower boundary  $y = 0$ ,  $0 \leq x \leq 1$ , and the upper one  $y = 1$ ,  $0 \leq x \leq 1$ , Dirichlet conditions are assigned. We impose Neumann conditions on the remaining boundaries. In Fig. 3(a), the relative  $L^\infty$ -convergence of numerical solution is shown when the node distribution is uniform, and we use  $m = 2$ . The convergence order seems to be  $O(\rho_\Omega^2)$ . Fig. 3(b) illustrates the perfectly reproducing property for polynomial solution, even on randomly distributed nodes when we use  $m = 3$ , which should be predictable from the reproducing properties of FMLSrk operators.

Now, the proposed method is applied to the electrostatic problem on a complicated geometry with Dirichlet and Neumann boundary conditions. The geometry and the boundary conditions are shown in Fig. 4(a). Fig. 4(b) displays the nodes for electric potential computation that have a considerably irregular distribution with concentrations near tip regions of the electrodes. In this case, we use the second-order basis polynomial in calculating shape functions, i.e.,  $m = 2$ . The conjugate gradient method (CGM) for the discretized non-symmetric system is adopted. The number of CGM iterations for this problem with 4159 nodes is around 1108 to achieve the successive tolerance up to order  $O(10^{-8})$ , which implies that the stiffness matrix is well conditioned. The elapsed CPU time on a Pentium 4 for solving this problem is about 120 s. However, 100 s of the 120 are purely devoted to automatically calculating the shape function values at the given nodes, which can be seen as a counterpart, replacing the task of mesh or grid generation. Fig. 4(c) and (d) illustrates the equipotential lines and the electric vector field at the sample points, respectively, using the approximation formula (18). The computational results apparently reveal the capabilities of the point collocation method combined with dilation function, in spite of the geometric singularity.

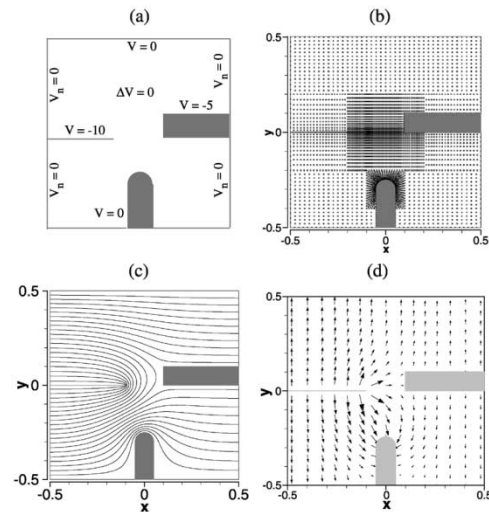


Fig. 4. (a) Configuration of electric potential problem. (b) Irregular node distribution (4159 nodes). (c) Contour plot of the computed electric potential  $V(x, y)$ . (d) Electric field computation of  $\nabla V(x, y)$  when  $m = 2$ .

tion method combined with dilation function, in spite of the geometric singularity.

## VI. CONCLUSION

The point collocation method, which was based on the FMLSrk operators presented in this paper, was proposed. We introduced the notion of dilation function and furthermore designed a procedure to construct a continuous dilation function. With this dilation function, we performed the electric field computation on irregular nodes distributed in a complicated geometry. The stepping node distributions are allowed in calculating the numerical solution with the help of the dilation function construction algorithm. Developing a more flexible algorithm for the dilation function construction affects the accuracy and the stability of the point collocation method. Therefore, the point collocation method in this paper is a very promising truly mesh-free method that is applicable to other problems such as optimization problems, moving boundary problems, and so on. Especially for 3-D problems, it is expected to be a strong method for computational aspects.

## REFERENCES

- [1] P. Breitkopf, G. Touzot, and P. Villion, "Double grid diffuse collocation method," *Comput. Mech.*, vol. 25, pp. 199–206, 2000.
- [2] N. R. Aluru, "A point collocation method based on reproducing kernel approximations," *Int. J. Numer. Methods Eng.*, vol. 47, pp. 1083–1121, 2000.
- [3] Y. Luo and U. Häussler-Combe, "A generalized finite-difference method based on minimizing global residual," *Comput. Meth. Appl. Mech. Eng.*, vol. 191, pp. 1421–1438, 2002.
- [4] S. A. Viana and R. C. Mesquita, "Moving least square reproducing kernel method for electromagnetic field computation," *IEEE Trans. Magn.*, vol. 35, pp. 1372–1375, May 1999.
- [5] W. K. Liu, S. Li, and T. Belytschko, "Moving least square reproducing kernel methods (I) methodology and convergence," *Comput. Meth. Appl. Mech. Eng.*, vol. 143, pp. 422–433, 1996.
- [6] D. W. Kim and Y. Kim, "Point collocation methods using the fast moving least square reproducing kernel approximation," *Int. J. Numer. Methods Eng.*, vol. 56, pp. 1445–1464, 2003.